

Supporting Information

Comparison of Self-Assembled and Micelle Encapsulated QD Chemosensor Constructs for Biological Sensing

Christopher M. Lemon and Daniel G. Nocera*

Department of Chemistry and Chemical Biology, 12 Oxford Street, Harvard University, Cambridge, MA 02138, United States

dnocera@fas.harvard.edu

<i>Index</i>	<i>Page</i>
Materials	S2
NMR spectral details	S2
Corrole synthesis	S2
NMR spectra	S3
Figure S1. Absorption and emission spectra of 1	S7
Figure S2. Absorption and emission spectra of QD	S8
Figure S3. Bright field TEM images of QD	S9
Figure S4. Spectral changes associated with titration of QD with 10 Eq. of 2	S10
Figure S5. Spectral changes associated with titration of QD with 20 Eq. of 1	S11
Figure S6. Spectral overlap of QD emission and 1 absorption	S12
Figure S7. Excitation spectra of 1 , QD1 , and QD2	S13
Figure S8. Absorption and emission spectra of QD-MC	S14
Figure S9. Absorption spectra of QD1-MC and QD2-MC	S15
Figure S10. Spectral overlap of QD-MC emission and 1 absorption	S16
Table S1. Summary of binding constants	S17
Table S2. Summary of FRET parameters	S18

Materials

The following materials were used as received: dichloromethane (CH_2Cl_2), ethyl acetate (EtOAc), ethanol (EtOH), pyridine, inhibitor-free tetrahydrofuran (THF), toluene, 1,1',3,3',3'-hexamethylindotricarbocyanine iodide (HITCI), silica gel 60 Å 230–400 mesh from Sigma-Aldrich; sodium hydroxide (NaOH) and sodium sulfate (Na_2SO_4), from Mallinckrodt; gold(III) acetate ($\text{Au}(\text{OAc})_3$) and pyrrole from Alfa Aesar; argon, 1% O_2 /99% N_2 , 5% O_2 /95% N_2 , and 10% O_2 /90% N_2 gas from Airgas; chloroform-*d* (CDCl_3) from Cambridge Isotope Laboratories; Rhodamine 6G from Lambda Physik; HCl from EMD; 1,2-dioleoyl-*sn*-glycero-3-phosphoethanolamine-N-[methoxy(polyethylene glycol)-2000] ammonium salt, 25 mg/mL solution in chloroform from Avanti Polar Lipids; and Dulbecco's phosphate-buffered saline (PBS) without calcium and magnesium from GE Healthcare Laboratories. The free-base corrole 10-(4-methoxycarboxyphenyl)-5,15-bis(pentafluorophenyl)corrole (**H₃-2**)¹ were prepared according to literature methods. CdSe quantum dots overcoated with ZnS (**QD**) were prepared using modified literature methods.^{2,3} As synthesized, the surface (capping) ligands of the quantum dots are a mixture of oleic acid and oleylamine.

NMR Spectral Details

All ^1H NMR spectra were recorded in CDCl_3 at 23 °C at 500 MHz. These spectra are presented on pages S4–S6.

Corrole Synthesis

10-(4-Carboxyphenyl)-5,15-bis(pentafluorophenyl)corrole (H₃-1**).** In a 10 mL microwave tube, 100 mg (0.13 mmol) of 10-(4-methoxycarboxyphenyl)-5,15-bis(pentafluorophenyl)corrole (**H₃-2**) was dissolved in 2 mL of inhibitor-free THF and 2 mL of 6 M NaOH was added. The biphasic mixture was irradiated at 80 °C in a microwave reactor (CEM Discover) for 18 h. Concentrated HCl was added to the reaction mixture until the pH was acidic, as measured using pH paper, and subsequently stirred at room temperature for 1 h. The crude reaction mixture was extracted into CH_2Cl_2 ($\times 4$); the combined organics were washed with water then dried over Na_2SO_4 . Solvents were removed by rotary evaporation to afford 84 mg (86 % yield) of the product as a violet solid. The compound was pure by ^1H NMR and was used without further purification. ^1H NMR (500 MHz, CDCl_3) δ 8.29 (d, J = 7.7 Hz, 2H), 8.51 (d, J = 8.0 Hz, 2H), 8.56 (d, J = 4.0 Hz, 2H), 8.67 (d, J = 4.7 Hz, 2H), 8.74 (d, J = 4.5 Hz, 2H), 9.08 (d, J = 4.2 Hz, 2H).

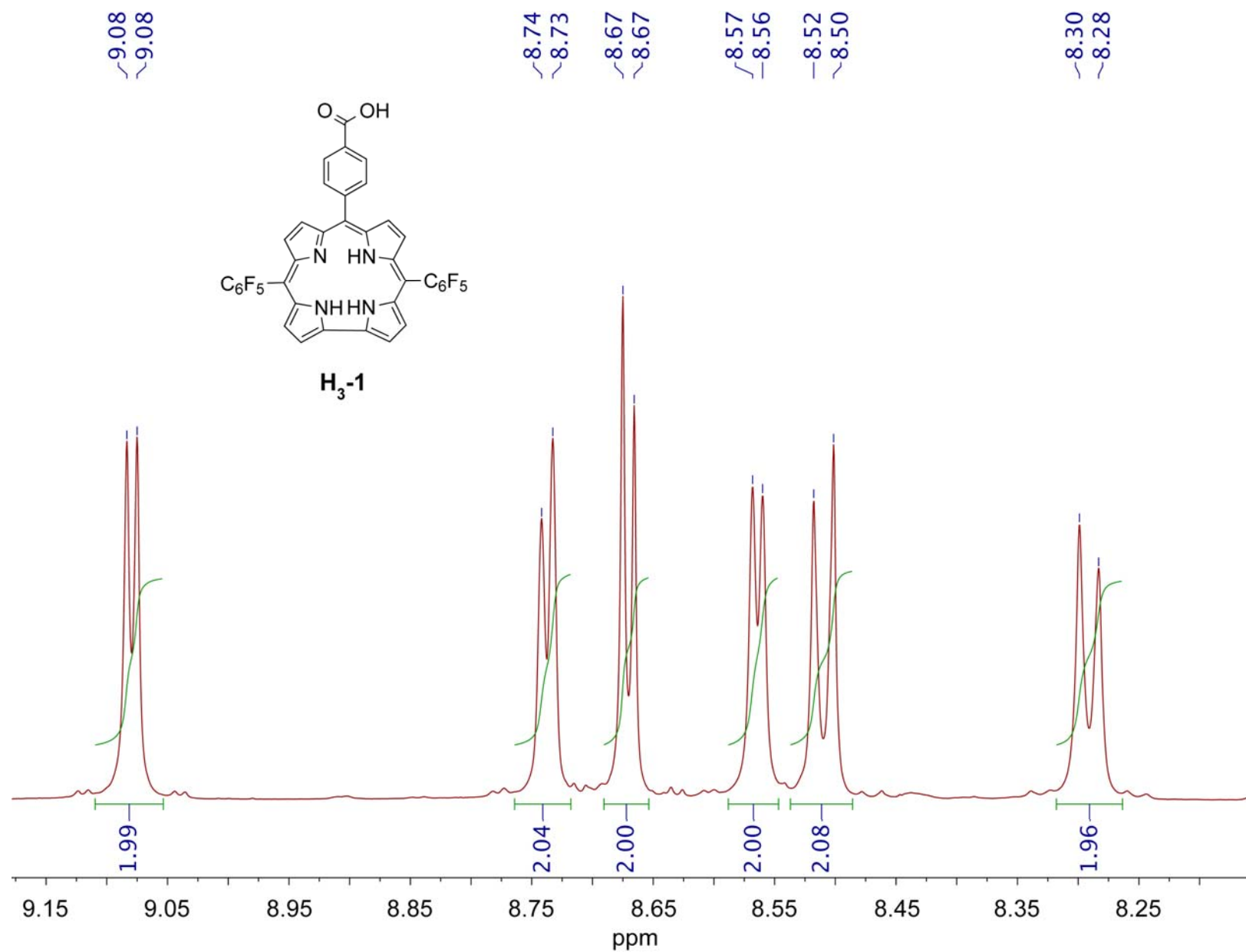
1 C. M. Lemon, R. L. Halbach, M. Huynh and D. G., Nocera, *Inorg. Chem.* 2015, **54**, 2713–2725.

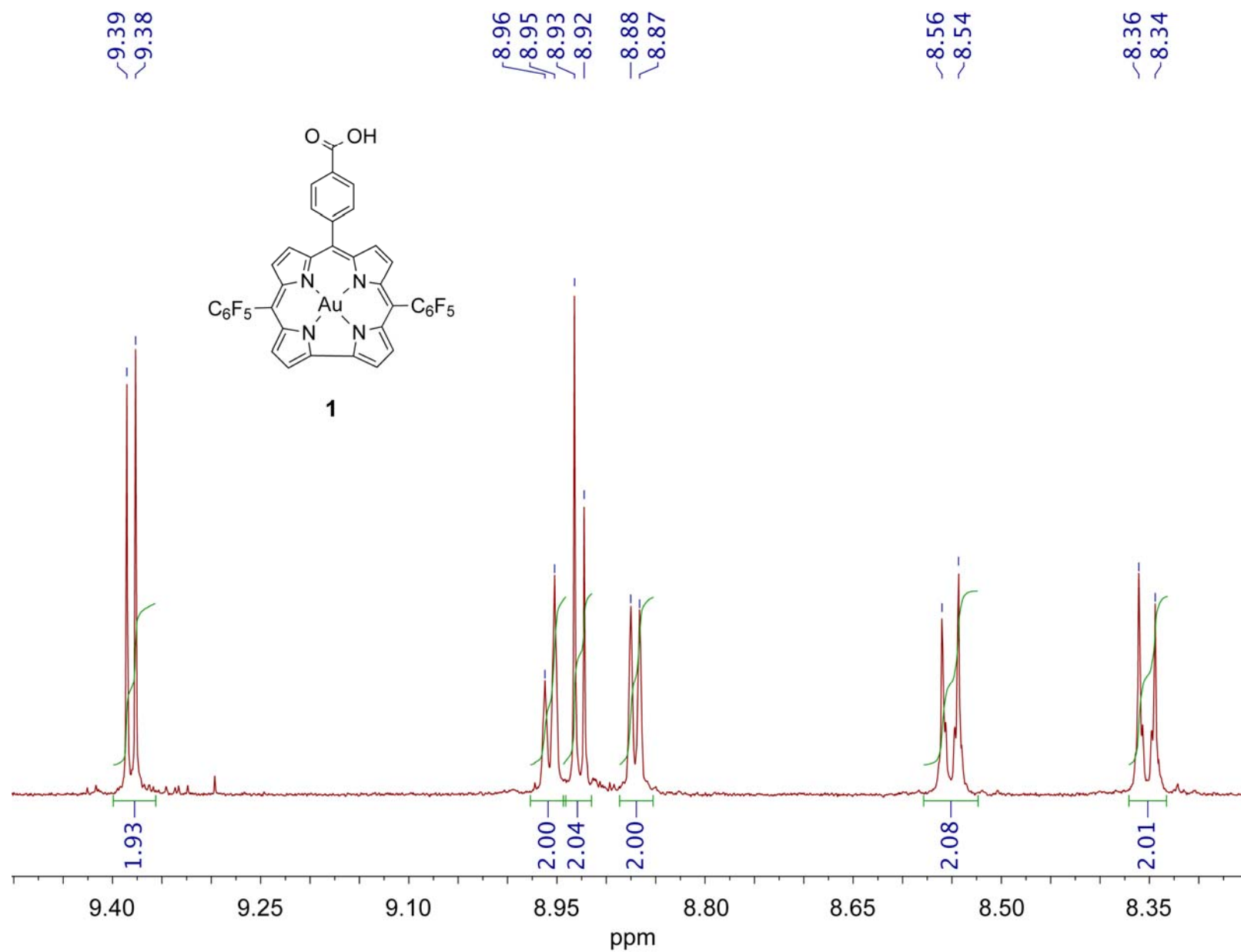
2 Z. A. Peng and X. Peng, *J. Am. Chem. Soc.*, 2001, **123**, 1389–1395.

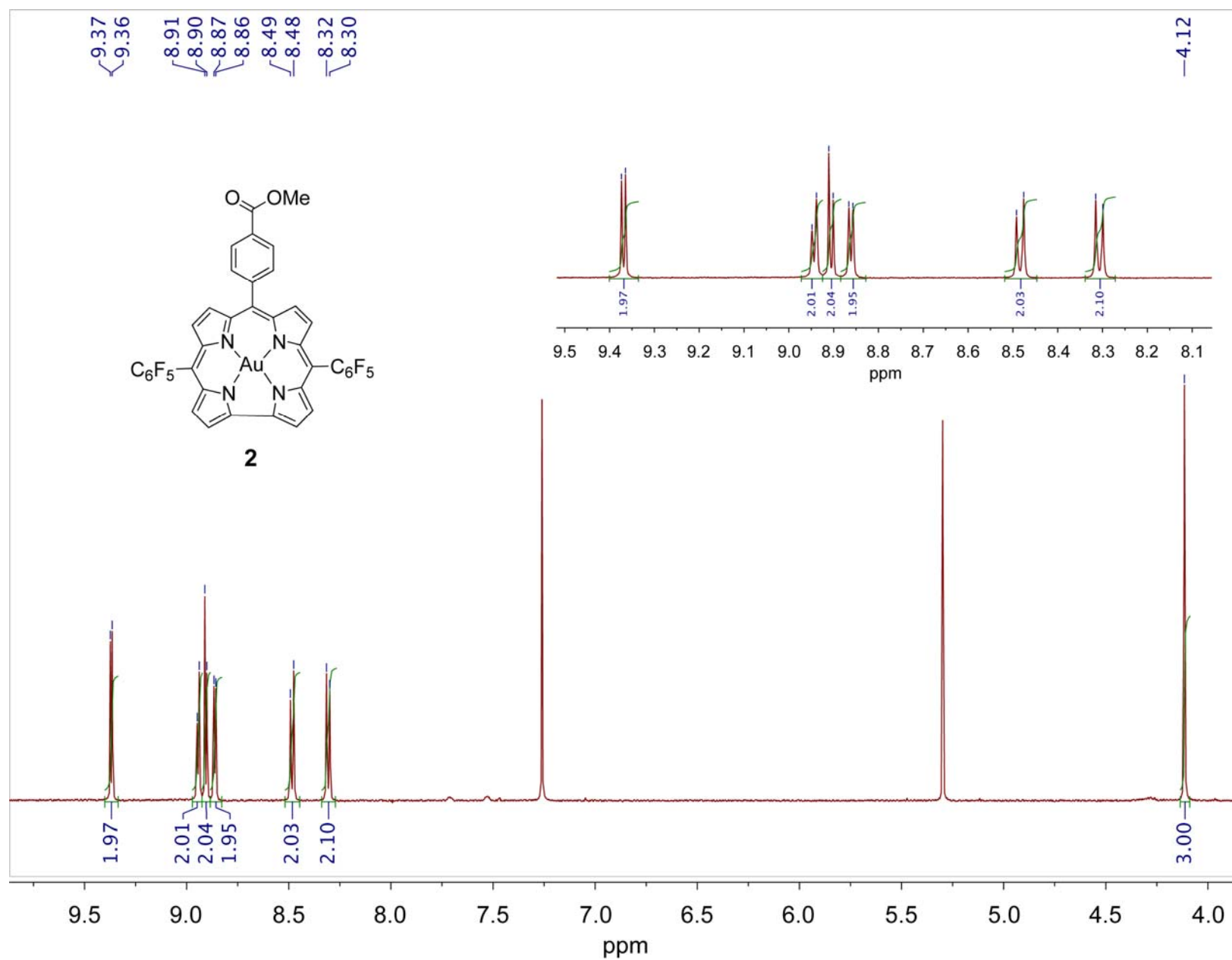
3 B. O. Dabbousi, J. Rodriguez Viejo, F. V. Mikulec, J. R. Heine, H. Mattoussi, R. Ober, K. F. Jensen and M. G. Bawendi, *J. Phys. Chem. B*, 1997, **101**, 9463–9475.

10-(4-Carboxyphenyl)-5,15-bis(pentafluorophenyl)corrolatogold(III) (1). In a 10 mL microwave tube, 84 mg (0.11 mmol) of the free-base corrole **H₃-1** was dissolved in 5 mL of pyridine and 232 mg (0.62 mmol) of Au(OAc)₃ was added. The resultant mixture was stirred at room temperature overnight, protected from light. The crude reaction mixture was filtered over a plug of silica and rinsed with CH₂Cl₂ and then EtOAc; the collected filtrate was brought to dryness. The residue was purified on a silica gel column packed with CH₂Cl₂, using 1:1 CH₂Cl₂/EtOAc as the eluent. Solvent was removed to afford 34 mg of a red solid (32% yield). ¹H NMR (500 MHz, CDCl₃) δ 8.35 (d, *J* = 8.0 Hz, 2H), 8.55 (d, *J* = 8.2 Hz, 2H), 8.87 (d, *J* = 4.5 Hz, 2H), 8.93 (d, *J* = 4.9 Hz, 2H), 8.96 (d, *J* = 5.0 Hz, 2H), 9.38 (d, *J* = 4.5 Hz, 2H).

10-(4-Methoxycarbonylphenyl)-5,15-bis(pentafluorophenyl)corrolotogold(III) (2) In a 50 mL round bottom flask, 60 mg (0.078 mmol) free-base corrole **H₃-2** was dissolved in 5 mL pyridine, and 143 mg (0.382 mmol) Au(OAc)₃ was added. An additional 5 mL pyridine was added to rinse the solids into the flask. The solution was then stirred at room temperature, protected from ambient light. The crude reaction mixture was filtered over a plug of Celite and rinsed with CH₂Cl₂. Solvent was removed by rotary evaporation. The residue was purified on a silica gel column packed with hexanes, using 1:1 hexanes:CH₂Cl₂ as the eluent; the desired product eluted as a red solution. The title compound was isolated in 23% yield (17 mg) as a red solid. ¹H NMR (500 MHz, CDCl₃) δ 4.12 (s, 3H), 8.31 (d, *J* = 8.0 Hz, 2H), 8.49 (d, *J* = 8.0 Hz, 2H), 8.87 (d, *J* = 4.6 Hz, 2H), 8.91 (d, *J* = 4.9 Hz, 2H), 8.94 (d, *J* = 4.9 Hz, 2H), 9.38 (d, *J* = 4.5 Hz, 2H).







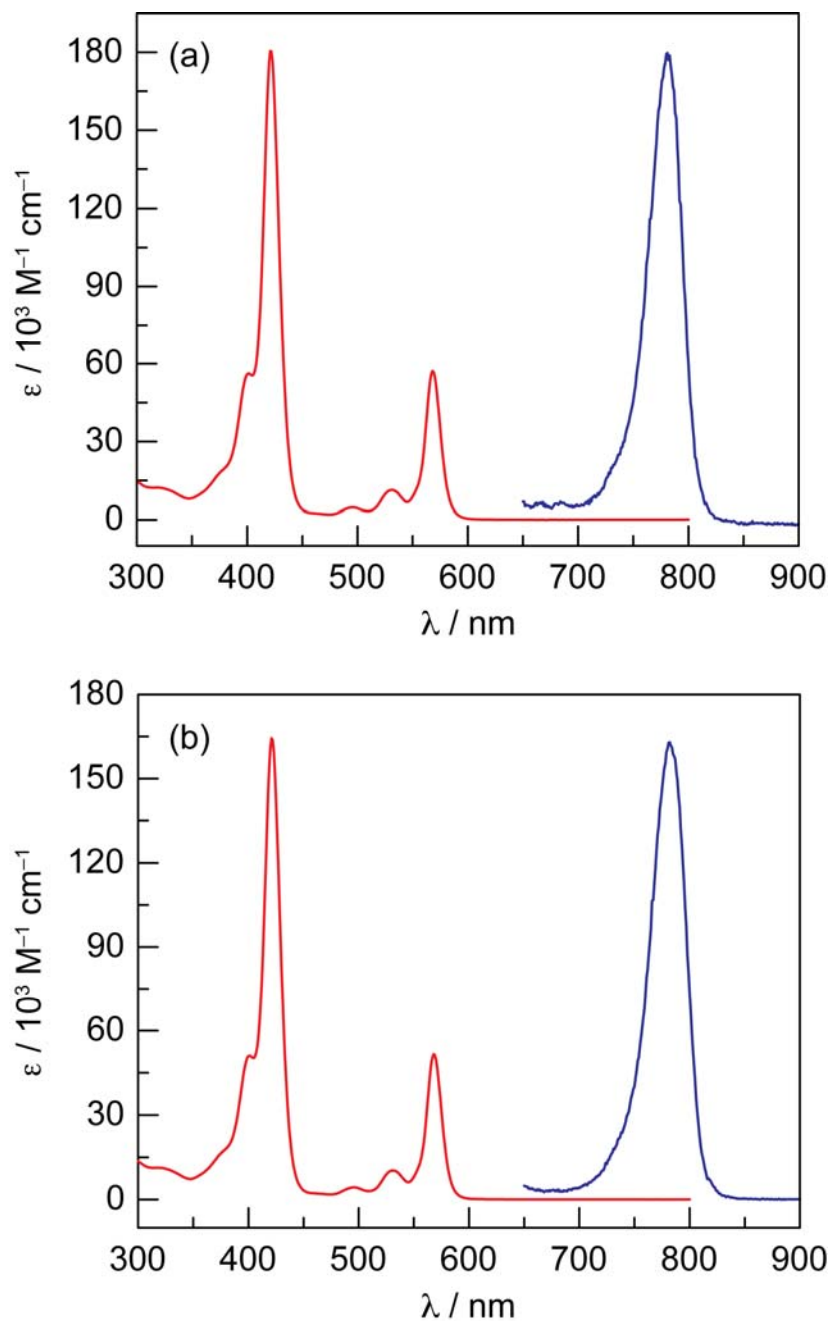


Figure S1. Steady-state absorption spectrum (—) of compounds (a) **1** and (b) **2** in toluene. The major absorption features are: B(1,0) at 401 nm, B(0,0) at 421 nm, Q(2,0) at 496 nm, Q(1,0) at 531 nm, and Q(0,0) at 568 nm. These absorption maxima are identical for both compounds **1** and **2**. The emission spectra (—) ($\lambda_{\text{exc}} = 570 \text{ nm}$) were recorded for freeze-pump-thawed samples in toluene and exhibit the T(0,0) phosphorescence transition at 781 nm and 780 nm for **1** and **2**, respectively.

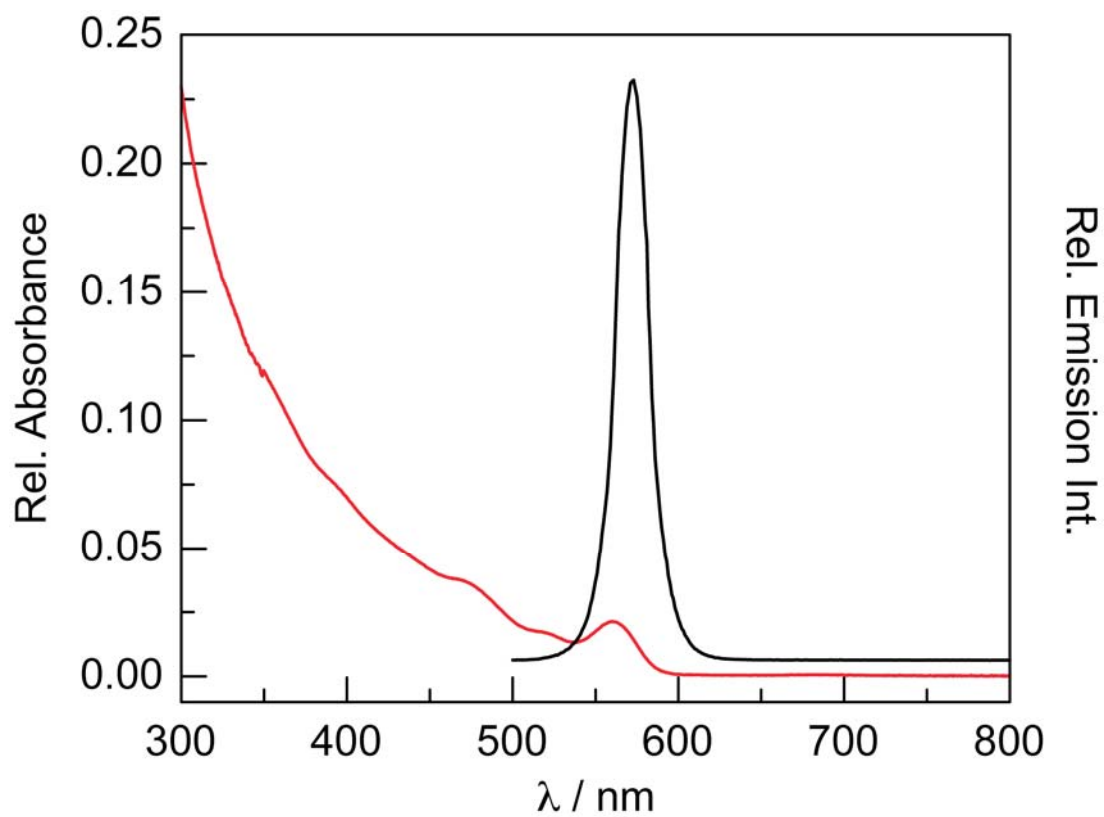


Figure S2. Steady-state absorption (—) and emission (—) spectra ($\lambda_{\text{exc}} = 470$ nm) of **QD** in toluene. This QD has a first absorption feature at 562 nm and the photoluminescence band is centered at 572 nm.

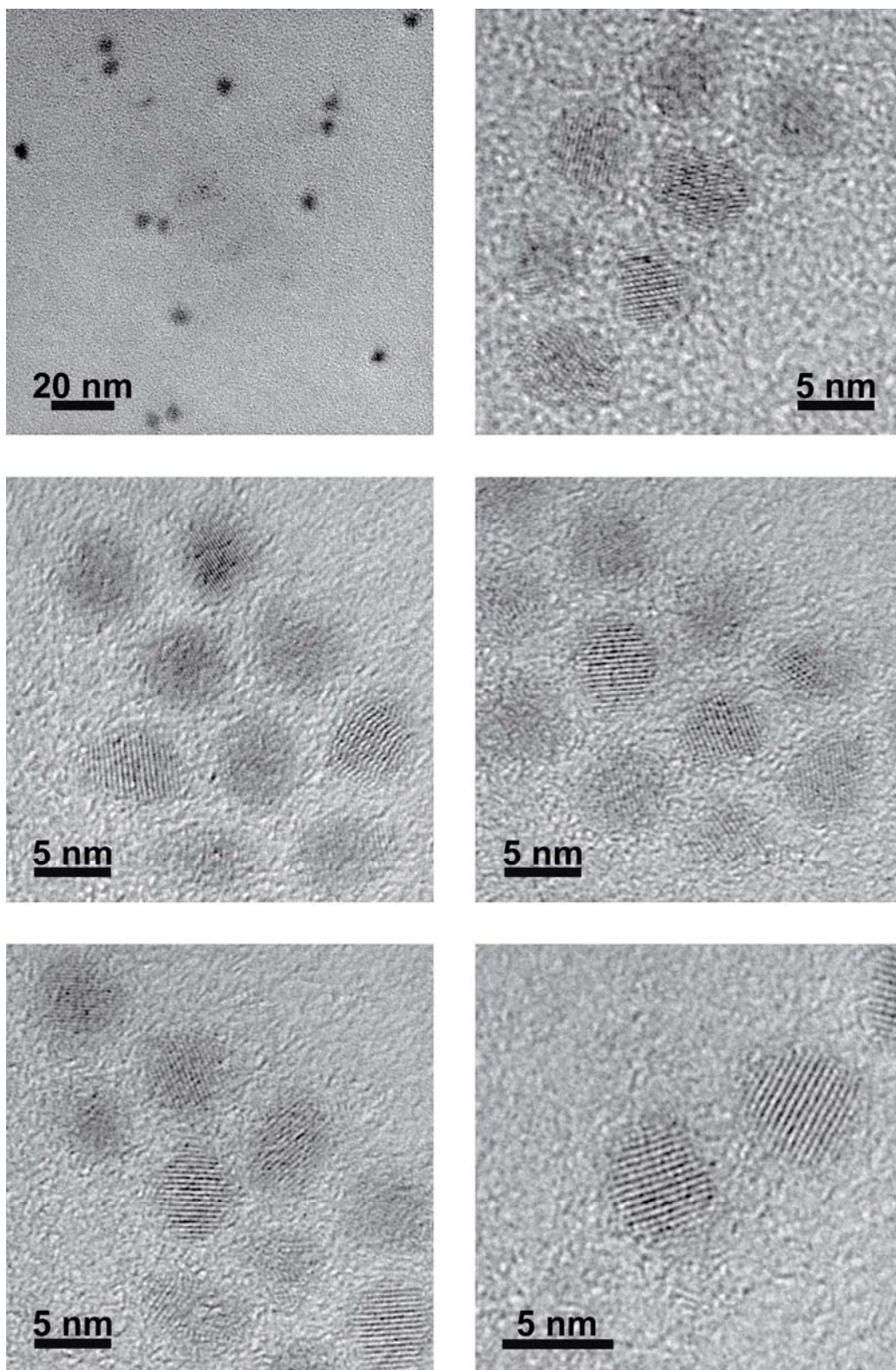


Figure S3. Representative bright field TEM images of **QD**.

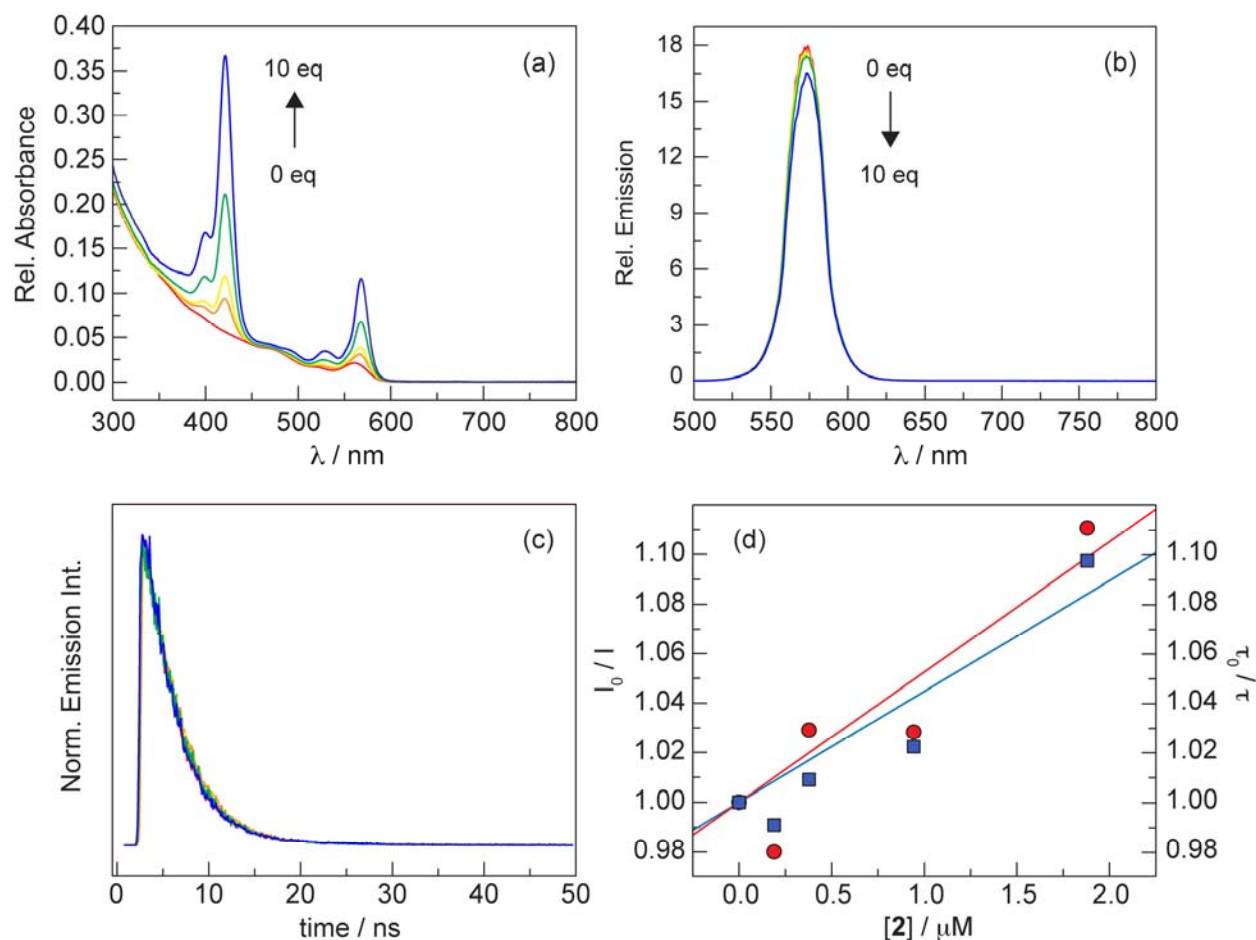


Figure S4. Spectral changes associated with the titration of a toluene solution of QD (—) with 1 (—), 2 (—), 5 (—), and 10 (—) equivalents of 2. (a) The intensity of the Soret and Q bands of the corrole increases. (b) The QD emission ($\lambda_{\text{exc}} = 470$ nm) intensity, as well as the photoluminescence decay traces (c) of QD lifetime ($\lambda_{\text{exc}} = 480$ nm) remain largely unperturbed with increasing concentration of 2. (d) Stern-Volmer plot to determine the equilibrium binding constant using both intensity data (■) from (b) and lifetime data (●) from (c) to give K_A values of $4.47 \times 10^4 \text{ M}^{-1}$ and $5.25 \times 10^4 \text{ M}^{-1}$, respectively.

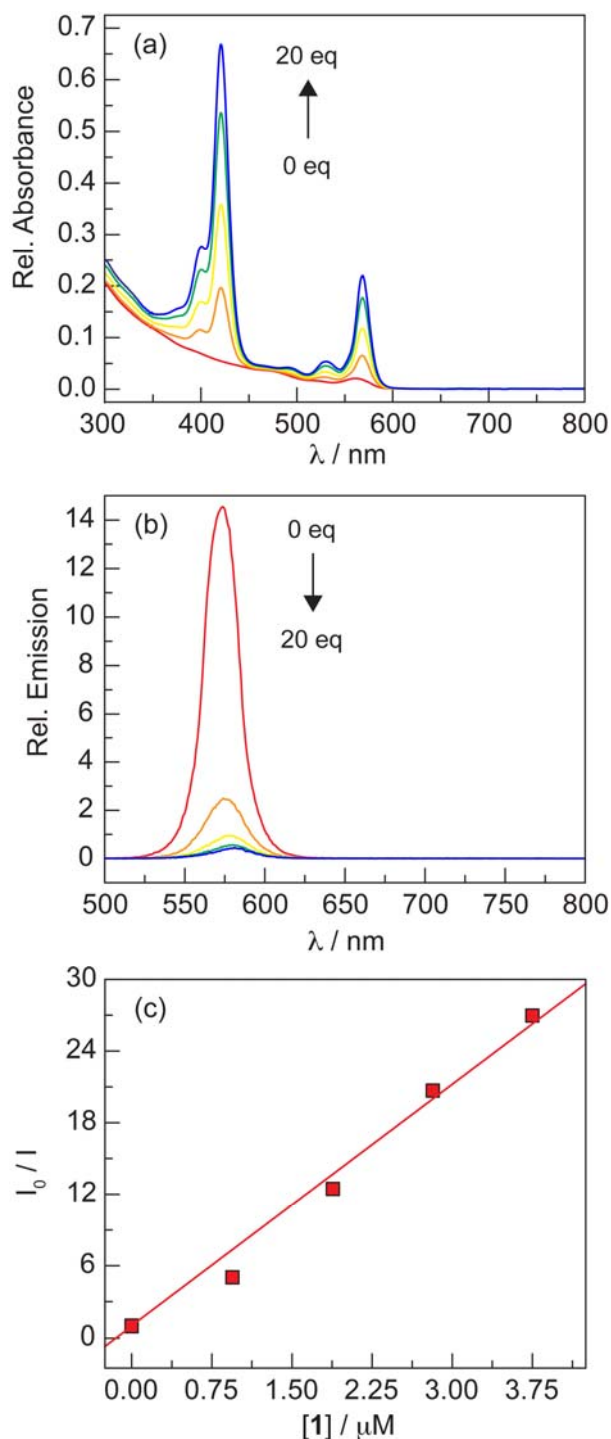


Figure S5. Spectral changes associated with the titration of a toluene solution of **QD** (—) with 5 (—), 10 (—), 15 (—), and 20 (—) equivalents of **1**. (a) The intensity of the Soret and Q bands of the corrole increase. (b) The QD emission ($\lambda_{\text{exc}} = 470 \text{ nm}$) intensity decreases with increasing concentration of **1**. (c) Stern-Volmer plot to determine the equilibrium binding constant using the intensity data (■) from (b) to give K_A value of $6.74 \times 10^6 \text{ M}^{-1}$. This data demonstrates that binding saturation is not observed up to 20 equivalents of **1**.

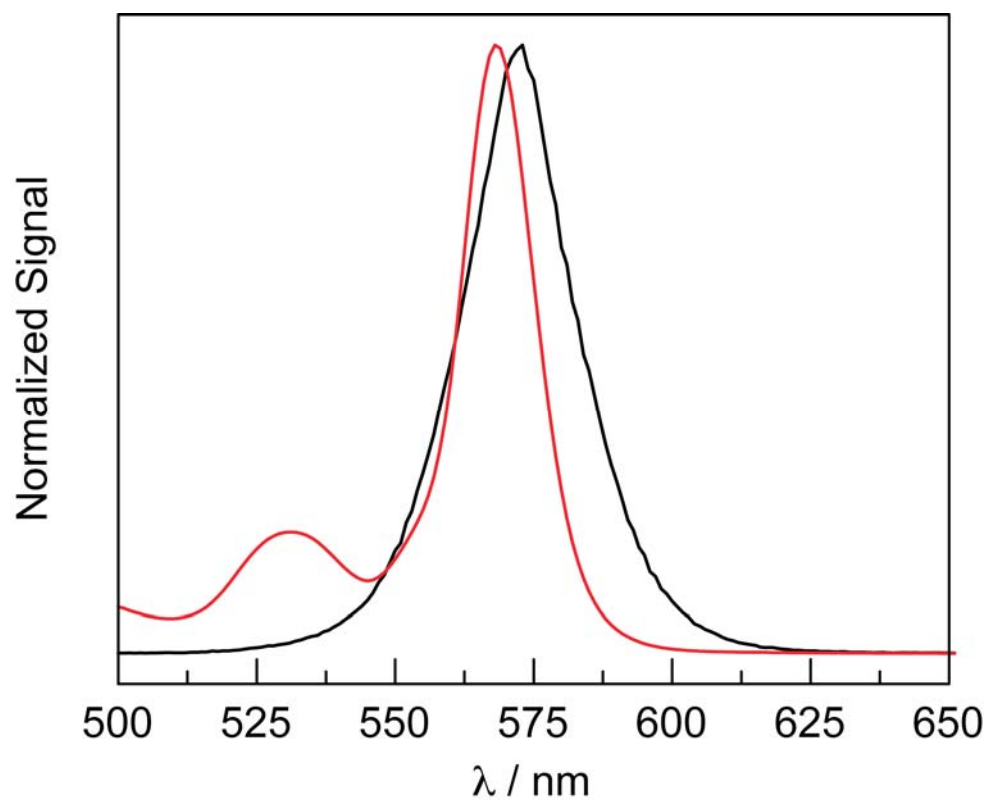


Figure S6. Normalized emission of **QD** (—) ($\lambda_{\text{exc}} = 470$ nm) and absorption of **1** (—), illustrating the spectral overlap that accounts for the FRET efficiency in **QD1**.

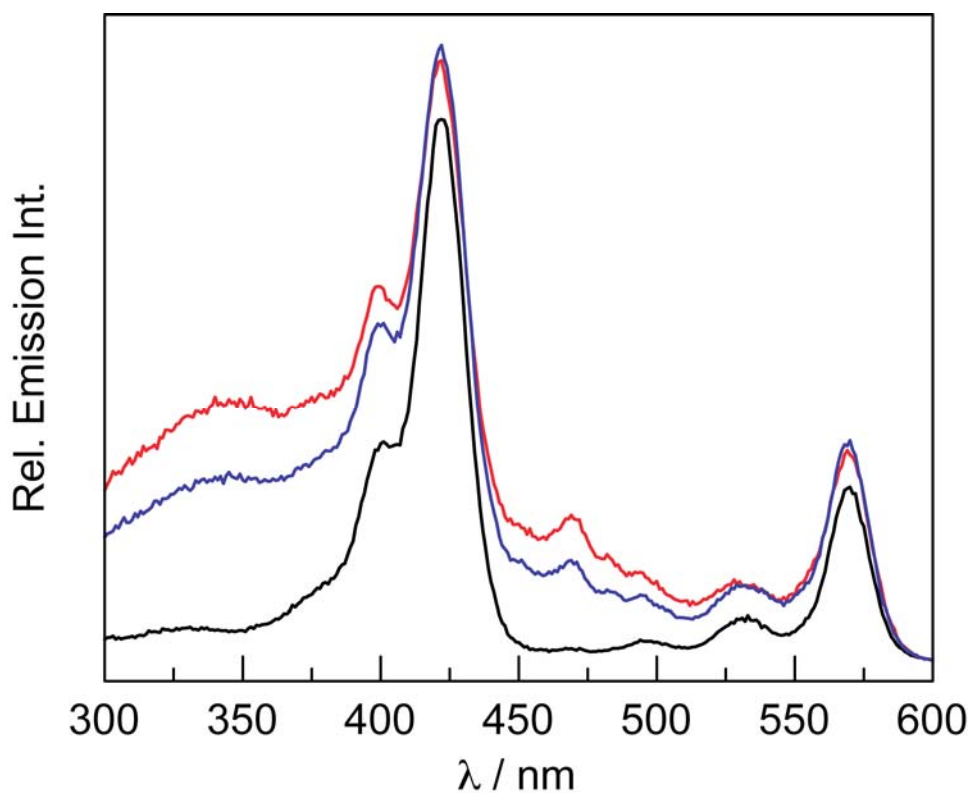


Figure S7. Excitation spectra ($\lambda_{\text{em}} = 780 \text{ nm}$) of concentration matched solutions of **1** (—), **QD1** (—), and **QD2** (—) in toluene. Excitation light was removed using a 610 nm long pass filter. **QD1** and **QD2** show increased emission intensity at $\lambda < 375 \text{ nm}$ relative to **1**. In this region, QD absorption dominates, indicating that it is the donor in the FRET process.

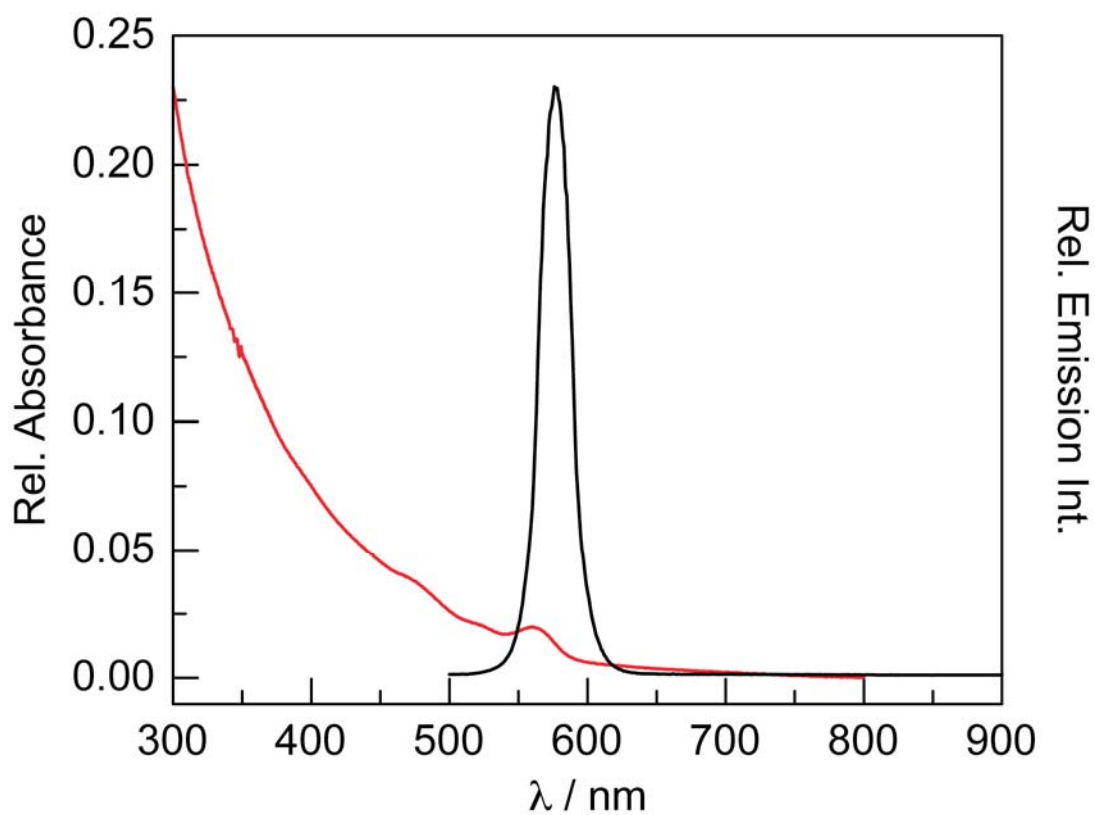


Figure S8. Steady-state absorption (—) and emission (—) spectra ($\lambda_{\text{exc}} = 470$ nm) of **QD-MC** in PBS. This QD has a first absorption feature at 564 nm and the photoluminescence band is centered at 575 nm.

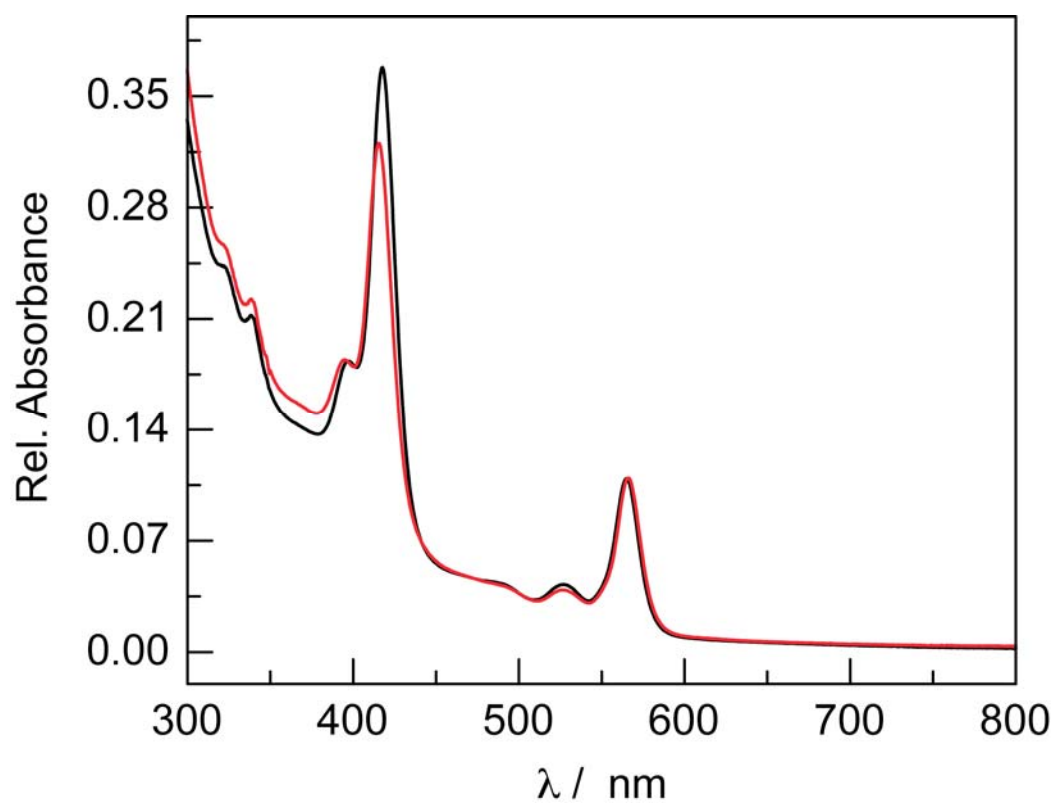


Figure S9. Steady-state absorption spectra of **QD1-MC** (—) and **QD2-MC** (—) in PBS.

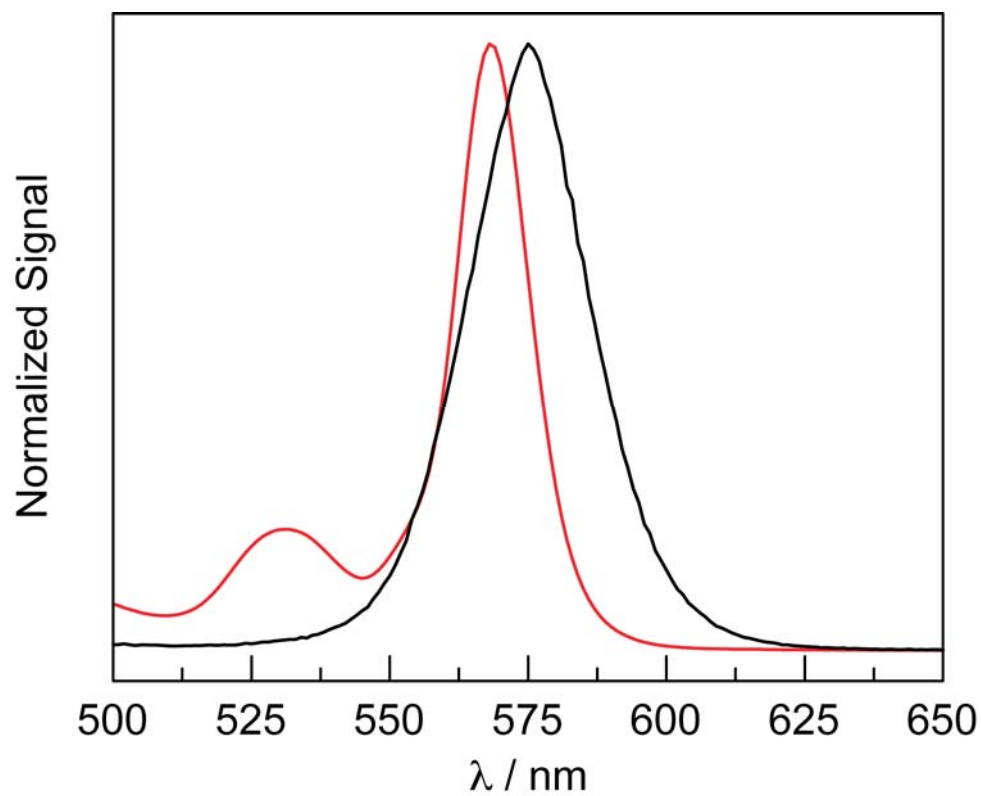


Figure S10. Normalized emission of **QD-MC** (—) ($\lambda_{\text{exc}} = 470 \text{ nm}$) and absorption of **1** (—), illustrating the spectral overlap that accounts for the FRET efficiency in **QD1-MC**.

Table S1. Summary of binding constants of **1** and **2** with **QD**

Compound	K_A Intensity^a (M⁻¹)	K_A Lifetime^b (M⁻¹)
1	$2.18 \pm 0.61 \times 10^6$	$1.05 \pm 0.30 \times 10^6$
2	4.47×10^4	5.25×10^4

^a Determined using QD emission intensity data, ^b Determined using QD emission lifetime data

Table S2. Summary of FRET Parameters

Construct	m	J^a (M ⁻¹ cm ⁻¹)	R_0^a (nm)	r^b (nm)	E ^c
QD1	10	3.08×10^{-13}	5.12	5.70	0.84
QD1 _{2hv}	10	3.08×10^{-13}	5.12	4.88	0.93
QD2	10	2.77×10^{-13}	5.03	9.12	0.22
QD1-MC	10	2.69×10^{-13}	4.13	3.94	0.93
QD2-MC	9	2.42×10^{-13}	4.06	5.24	0.66

^a Calculated using Eq. 3, ^b Calculated using Eq. 1, ^c Calculated using Eq. 2